ACS OMEGA

Article

Cite This: ACS Omega 2017, 2, 8618−8624

Development of a Fluorogenic Reactivity Palette for the Study of Nucleophilic Addition Reactions Based on *meso*-Formyl BODIPY Dyes

Lana E. Greene, Richard Lincoln, Katerina Krumova, and Gonzalo Cosa*

Department of Chemistry and Center for Self Assembled Chemical Structures, McGill University, 801 Sherbrooke Street West, Montreal, Quebec H3A 0B8, Canada

Supporting Information

ABSTRACT: We describe herein a fluorescence-based assay to characterize and report on nucleophilic addition to carbonyl moieties and highlight the advantages a fluorescence-based assay and multiplex analysis can offer. The assay relies on the fluorogenic properties of *meso*-formyl boron-dipyrromethene (BODIPY) dyes that become emissive following nucleophilic addition. A reactivity palette is assembled based on the increasing electrophilic character of five *meso*-formyl BODIPY compounds tested. We show that increasing rates of emission enhancement correlate with the decreasing electrophilic character of BODIPY dyes in the presence of an acid catalyst and a nucleophile. These results are consistent with the rate-limiting step involving activation of the electrophile. Increasing product formation is shown to correlate with the increasing electrophilic character of the BODIPY dyes, as expected based on thermodynamics. In addition to providing rates of reaction, analysis of the fluorescence parameters for the reaction mixtures, including emission quantum yields and fluorescence lifetimes, enables us to determine the extent of reactant conversion at equilibrium (in our case the estimated yield of a transient species) and the presence of different products, without the need for isolation. We anticipate that our reactivity palette approach, combined with the in-depth fluorescence analysis discussed herein, will provide guidelines toward developing fluorogenic assays of reactivity offering multiplex information, beyond fluorescence intensity.

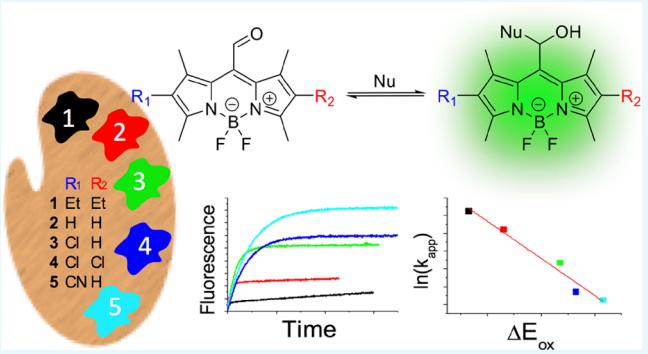

INTRODUCTION

A significant effort has been devoted over the past decade toward developing fluorogenic probes for reaction screening.[1−6] A number of fluorescence-based assays have been reported to monitor and study bond formation in a diverse set of reactions including aldol reactions,[7−9] Mannich-type reactions,[10] Michael additions,[11−13] and palladium-catalyzed reactions.[14−16] These assays, using fluorescence intensity as a marker, provide a rapid, in situ screening platform that is of simple application and requires minimum equipment investment.

We serendipitously uncovered that *meso*-formyl boron-dipyrromethene (BODIPY) dyes are nonemissive, yet their emission is readily restored following the reaction with methanol.[17,18] These dyes, we reasoned, would serve as uniquely sensitive probes of nucleophilic attack, given that their emission is undetectable before the reaction (i.e., their emission quantum yield is nominally 0) but readily observable to the naked eye upon methanol addition.[18] Given the ubiquitous nature of nucleophilic addition reactions in biology[19−22] and in synthesis, the availability of a series of fluorogenic electrophiles[23] would provide a simple, suitable tool to study nucleophile and aldehyde reactivity.

Here, we demonstrate that a reactivity palette may be assembled for nucleophilic addition screening composed of electrophilic fluorogenic *meso*-formyl BODIPY dyes of increasing reactivity. We show that the rates of emission enhancement and the emission intensity measured for *meso*-formyl BODIPY dyes upon hemiacetal and/or acetal formation in the presence of various small alcohols, water, and ethanedithiol (see Scheme 1) provide suitable markers to elaborate a reactivity scale and to determine the extent of

Scheme 1. Expected Products from the Reaction of *meso*-Formyl BODIPY and an Alcohol (ROH)

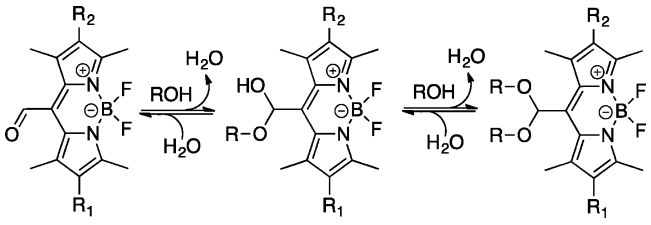

Received: November 14, 2017
Accepted: November 21, 2017
Published: December 4, 2017

DOI: 10.1021/acsomega.7b01795
ACS Omega 2017, 2, 8618−8624

reaction, respectively. We also highlight the valuable information a fluorescence assay may offer, with relative simplicity, beyond monitoring the fluorescence intensity alone. Specifically, we show the importance of monitoring the photophysical parameters of the reaction mixtures, including the emission quantum yield and the fluorescence lifetime, and of investigating the photophysical properties of the reaction products. Information on reaction yields, number of products, and type of products formed, we show, may be gained upon inspecting these various photophysical properties.

We propose that our reactivity palette approach combined with the in-depth fluorescence analysis developed herein will be of general applicability toward developing additional fluorogenic assays (including high throughput) on reactivity.

RESULTS AND DISCUSSION

Rationale. Toward implementing a reactivity scale, we conceived a fluorogenic reactivity palette consisting of five electrophilic, nonemissive, *meso*-formyl BODIPY dyes (see compounds **1**−**5**, Figure 1).[18] Nucleophilic addition and concomitant disruption of the formyl moiety deactivate an otherwise highly efficient nonradiative decay pathway for the excited state,[17,18] rendering the probes emissive (Figure 2A). *meso*-Formyl BODIPY dyes thus provide highly sensitive substrates toward developing a fluorogenic palette.

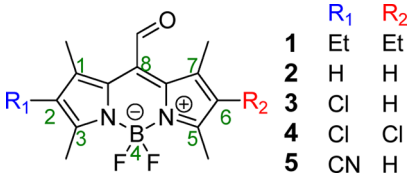

	R_1	R_2
1	Et	Et
2	H	H
3	Cl	H
4	Cl	Cl
5	CN	H

Figure 1. Structure of *meso*-formyl BODIPY dyes used in this work. The numbering of the BODIPY core is shown in green.

To tune the electrophilic character of BODIPY dyes, substitution of the BODIPY core was performed with either electron-rich or electron-withdrawing groups at positions C2 and C6 of the dye. From a frontier molecular orbital (FMO) perspective, the reaction of a formyl group with a nucleophile involves orbital mixing between the highest occupied molecular orbital of the nucleophile and the lowest unoccupied molecular orbital (LUMO) of the formyl group. Substitution of BODIPY dyes with electron-rich groups, destabilizing the LUMO, renders the formyl moiety less electrophilic. In turn, substitution by electron-withdrawing groups, for example, either chlorine atoms or nitriles, and concomitant lowering of the LUMO render the formyl group more susceptible to nucleophilic attack.

Reactivity. The reactivity of compounds **1**−**5** was tested in acetonitrile upon the addition of methanol where either a hemiacetal or acetal may form. Steady-state emission experiments were conducted where fluorescence intensity enhancement immediately following the addition of the nucleophile was monitored. Although a trend in reactivity was apparent from results with compounds **1**−**5**, we also noticed large variations in reruns of the experiments, possibly the result of traces of water affecting the ensuing kinetics of reaction. This observation prompted us to explore the addition of an acid catalyst in a controlled fashion working initially with compound **3**. We chose *p*-toluenesulfonic acid (*p*-TsOH) as an organic acid catalyst, as it is commonly used in the preparation of acetals.[24−26] Reproducible results with *p*-TsOH enabled us to learn the equilibrium position and to obtain initial rates of reaction under a range of conditions.

Consistent with the reversible nature of the methanol addition (see Scheme 1), reaction of increasing amounts of

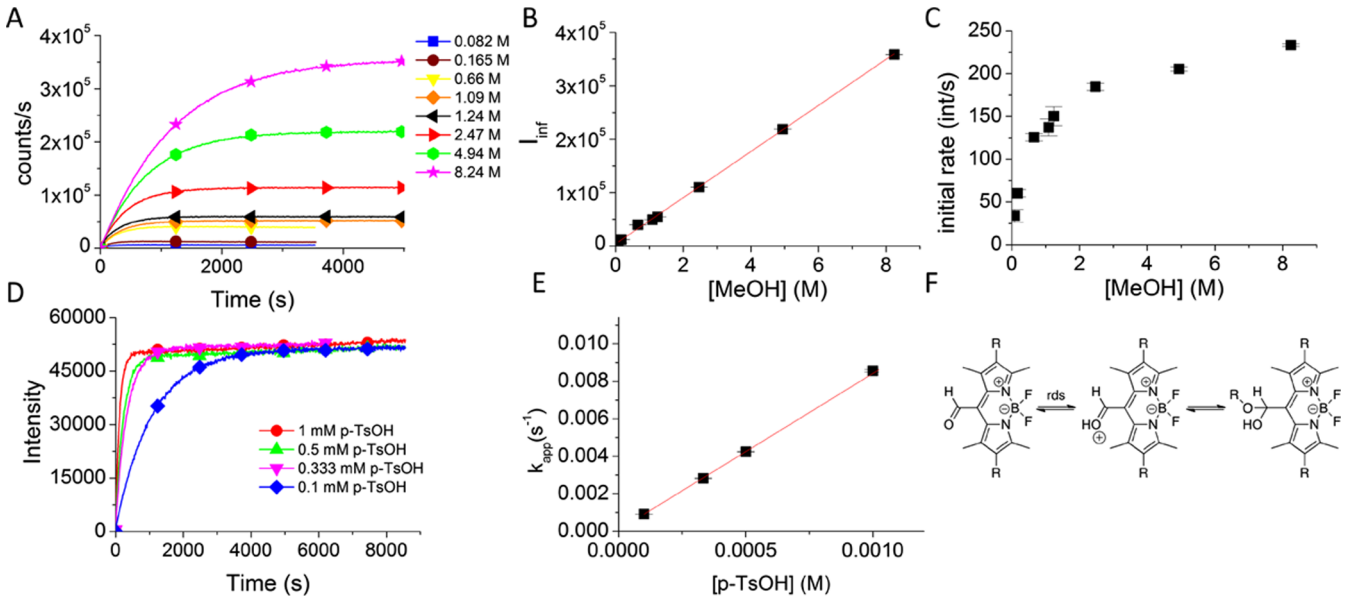

Figure 2. (A) Intensity−time trajectories following the reaction of **3** (4.5 μM) with increasing methanol concentration at 21 °C. (B) Correlation between the intensity at infinite time (I_∞) obtained from fitting the intensity−time trajectories in panel (A) using eq 2 and methanol concentration. (C) Relationship of the initial rate determined from panel (A) and methanol concentration. Error bars in *y* were obtained from the error associated with performing a linear fit on the initial increase of fluorescence enhancements in panel (A). (D) Intensity−time trajectories following the reaction of 4.5 μM of **3** with 1.09 M methanol in acetonitrile with varying concentrations of *p*-TsOH at 21 °C. (E) Correlation between the apparent rate constants for **3** obtained from fitting the trajectories displayed in panel (D) with eq 2 and *p*-TsOH concentration. Error bars were obtained from the error of the fitting with eq 2. (F) Equilibrium of *meso*-formyl BODIPY in the presence of an alcohol and an acid catalyst.

DOI: 10.1021/acsomega.7b01795
ACS Omega 2017, 2, 8618−8624

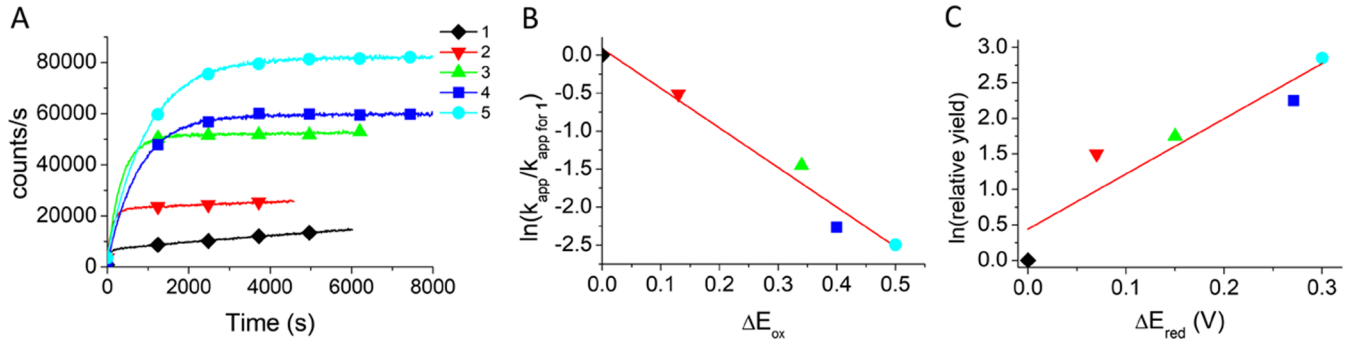

Figure 3. (A) Intensity−time trajectories following the reaction of compounds **1**−**5** with 1.09 M methanol in acetonitrile supplemented with 0.333 mM of *p*-TsOH at 21 °C. Dye concentrations were prepared such that their respective absorbance was 0.1 at the excitation wavelength used (i.e., 16, 20, 4.5, 16, and 3 μM for dyes **1**−**5**, respectively) (B) LFER correlation (slope = −5.2 and intercept = 0.1) between the ratio of apparent rate constants (k_{app}) and the difference in oxidation potentials (to compound **1**) in acetonitrile for BODIPY dyes **1**−**5** vs ferrocene previously obtained by us.[18] Where reversible oxidation potentials were not available (i.e., compounds **3**−**5**), anodic peak potentials were used. Compound **1** k_{app} and oxidation potentials were used as a reference. (C) LFER correlation (slope = 8 and intercept = 0.4) between the calculated relative yield (vide infra) and the difference in reversible reduction potentials in acetonitrile for dyes **1**−**5** (relative to compound **1**) measured vs ferrocene previously obtained by us.[18] Compound **1** yield and reduction potentials were used as a reference.

methanol at constant concentrations of compound **3** and in the presence of *p*-TsOH as a catalyst resulted in increased intensities at $t = \infty$, that is, once the reaction has reached equilibrium (see Figure 2A). Under the assumption that conversion of *meso*-formyl BODIPY is small (confirmed by the apparent fluorescence quantum yield experiments, vide infra) and working with a large excess of nucleophile, one may then obtain a linear correlation between the concentration of methanol added and the intensity at $t = \infty$ (Figure 2B). Under the above working conditions, both the electrophile initial concentration, $[E]_0$, and the nucleophile concentrations used, $[Nu]_0$, remain fairly constant upon reaction. One may then show that the electrophile−nucleophile adduct concentration [Nu−E], and thus the emission intensity, is proportional to the initial concentration of the reactants used (see eq 1).

$$K_{eq} = \frac{[Nu - E]}{[E]_0[Nu]_0} \quad (1)$$

In support of a pseudo-first-order reaction mechanism in the presence of excess nucleophile, the fluorescence intensity enhancement versus time curves followed an exponential behavior. Fitting the fluorescence intensity trajectories with an exponential growth curve according to kinetic eq 2 next enabled us to obtain values for the pseudo-first-order rate constant k_{app}, where I_∞ is the fluorescence intensity at $t = \infty$ once the reaction has reached equilibrium and I_0 is the fluorescence intensity at $t = 0$. To our initial surprise, while the initial rate of enhancement increased linearly with increasing methanol concentration, at a large excess of nucleophile, the reaction order changed and approached zero order on nucleophile concentration, as observed from the plateau in the plot of initial rate versus methanol concentration (see Figure 2C).

$$\frac{I_\infty - I_{(t)}}{I_\infty - I_0} = e^{-k_{app} \times t} \quad (2)$$

To understand the mechanism of the nucleophilic addition to compound **3**, we next subjected **3** to increasing concentrations of *p*-TsOH in the presence of large excess of nucleophile, 1.09 M methanol, where the reaction approaches zeroth order in methanol (see Figure 2D). A linear correlation was observed between the concentration of *p*-TsOH and the apparent rate constant (Figure 2E). The linearity suggests the formation of a catalyst-activated aldehyde (protonation of the *meso*-formyl BODIPY) as the rate-determining step and thus a general acid catalysis mechanism (see Figure 2F).

To test the reactivity of our palette, we monitored the rates of intensity enhancement for compounds **1**−**5** in acetonitrile in the presence of 1.09 M methanol and 0.333 mM *p*-TsOH (see Figure 3A). A linear free-energy relationship (LFER) analysis was conducted utilizing the natural logarithm of the ratio of measured apparent rate constant values (obtained according to eq 2, relative to compound **1**) and the difference in oxidation potentials for compounds **1**−**5** (see Figure 3B).[27]

Consistent with a rate-limiting step involving activation via protonation of *meso*-formyl BODIPY, we retrieved a negative slope for the LFER correlation. Electron-rich groups on the BODIPY core stabilize the activated complex, whereas the larger electronic density in the BODIPY core increases the basicity and stabilizes the protonated *meso*-formyl BODIPY dye. An energy increasing by ca. 0.5 eV (~48 kJ/mol) for the oxidation potential of BODIPY dyes previously obtained by us[18] in moving from electron-releasing ethyl groups (compound **1**) to an electron-withdrawing nitrile group (compound **5**) resulted in a drop by ca. 1 order of magnitude at 21 °C for rate constants. The rate enhancement observed with decreasing oxidation potential is smaller than 8 orders of magnitude expected at room temperature based on energy stabilization alone. This indicates that the *meso*-formyl moiety, which is uncoupled from the BODIPY core as it is 90° from the BODIPY plane,[17] is only moderately affected by the substitution of the BODIPY core.

To test the equilibrium position, we next compared the calculated relative yield of the emissive product (vide infra) obtained for compounds **1**−**5**, following the reaction with methanol. In comparing the percent yield, we assumed that the radiative decay constant (k_{rad}) for each of the hemiacetal products formed with compounds **1**−**5** was similar as is generally the case for BODIPY dyes and is the case for *meso*-hydroxymethyl BODIPY dyes obtained, following the reduction of the formyl moiety.[18]

DOI: 10.1021/acsomega.7b01795
ACS Omega 2017, 2, 8618−8624

A new LFER with a positive slope was obtained when correlating the natural logarithm of the ratio of the yield of the emissive product (relative to compound **1**) for dyes **1**−**5** in the presence of 1.09 M methanol and *p*-TsOH versus the difference in reduction potentials (relative to compound **1**) (LUMO energy values) (see Figure 3C). This LFER indicates that BODIPY cores bearing electron-withdrawing groups favor product formation. The results are consistent with FMO considerations, predicting the equilibrium position to be displaced toward products in the increasing order **1** < **2** < **3** < **4** < **5**. A 10-fold increase in the product formation was recorded upon stabilizing the LUMO by ca. 0.3 eV (29 kJ/mol) at 21 °C.

We next tested the effect of nucleophiles on the rate of addition to our formyl dyes by monitoring compound **3** in the presence of various small alcohols, water, and ethanedithiol (Figure 4). The formation of nonemissive *meso*-imines upon

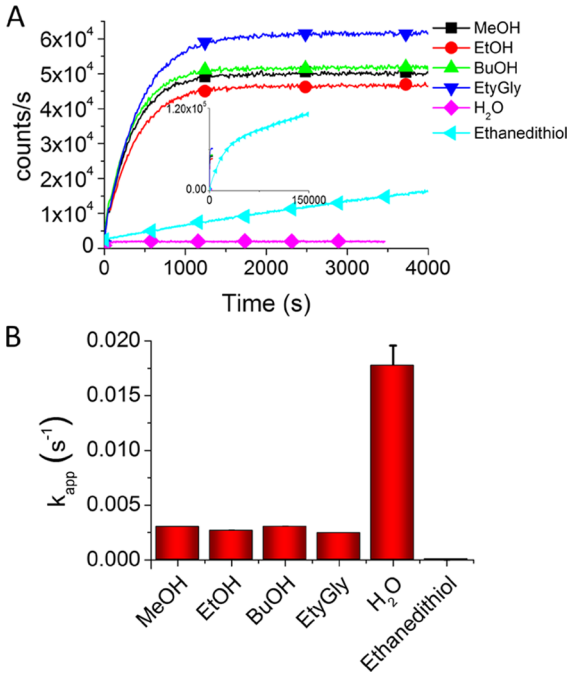

Figure 4. (A) Intensity−time trajectories following the reaction of 4.5 μM of compound **3** and 1.09 M methanol (MeOH), ethanol (EtOH), butanol (BuOH), ethylene glycol (EtyGly), water (H_2O), and ethanedithiol ($EtSH_2$) at 21 °C in acetonitrile supplemented with 0.333 mM of *p*-TsOH. (B) Apparent rate constants for various nucleophiles tested were obtained from fitting the intensity−time trajectories in panel (A) with eq 2. Error bars were obtained from the error of the fitting with eq 2.

the reaction of compounds **1**−**5** with amines precluded testing with this nucleophile substrate.[17] Furthermore, amines are known to be fluorescence quenchers of BODIPY dyes.[28] All alcohols tested reacted at comparable rates ($k_{app} \approx 0.003$ s^{-1}) and reached comparable fluorescence intensities (~50 000 counts/s). This is not surprising given the general acid catalysis mechanism proposed (vide supra). We did observe however a ca. −10-fold rate increase upon the use of water as a nucleophile which may be partly due to lowering of the pK_a of *p*-TsOH in the presence of water versus acetonitrile.[29,30] The hydrate formation led to a very small emission enhancement, indicating that it is not a stable compound.

A ~10-fold drop in the reaction rate was recorded upon the addition of ethanedithiol. The mismatch between the hard electrophile (formyl moiety) and the soft nucleophile (thiol) may alter the mechanism of the reaction, rendering the nucleophilic attack the rate-determining step. We also observed a ca. 2-fold larger emission enhancement in the presence of ethanedithiol consistent with the larger stability of thioacetals (and presumably hemithioacetals) versus acetals (and hemiacetals).[31]

Equilibrium. To determine the product(s) formed in the reactions of our palette with various alcohol nucleophiles, we prepared and isolated the *meso*-acetal BODIPY **6** from its precursor **5** (Figure 5A) by stirring at 80 °C with ethylene

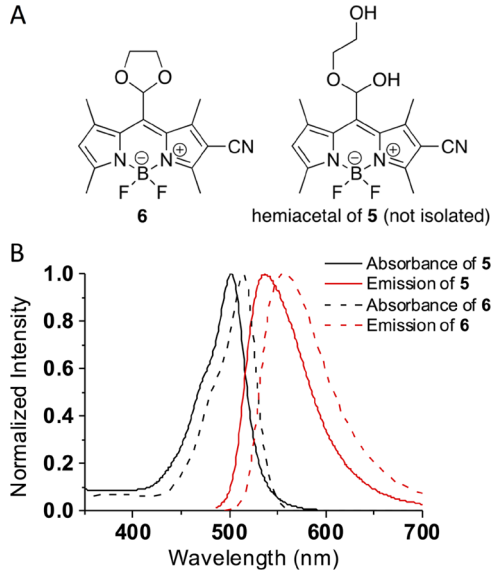

Figure 5. (A) Structure of compound **6** and the proposed structure of the major product of **5** dissolved in ethylene glycol. (B) Absorption and emission spectra of **5** and **6** dissolved in ethylene glycol.

glycol in the presence of *p*-TsOH. Figure 5B shows the absorption and emission spectra of acetal **6** in ethylene glycol in comparison to those of **5** dissolved in ethylene glycol, where the hemiacetal and acetal may both form. The absorption and emission maxima of **5** (reacted) and **6** in this solvent were markedly different (λ_{abs} = 502 nm and λ_{em} = 537 nm versus λ_{abs} = 514 nm and λ_{em} = 556 nm, respectively). The marked difference recorded between the spectra of the isolated acetal and the product obtained upon the addition of ethylene glycol to compound **5** highlights the predominant formation of hemiacetal (rather than acetal) in solutions of compound **5** in acetonitrile in the presence of either methanol or other alcohols studied herein (vide supra). In addition, fluorescence lifetimes of **5** and **6** were markedly different in ethylene glycol (Table S1). A similar conclusion would also apply to reactions with less electrophilic compounds **1**−**4**. Importantly, the poor solubility of compounds **1**−**5** in acetonitrile/methanol mixtures precluded the use of NMR toward monitoring the reaction mixture.

Photophysics of Reaction Mixtures. We next revisited the final intensities reached at equilibrium for various nucleophiles and compounds **1**−**5** studied herein to extract information on yields. In addition to providing a qualitative understanding on the extent of reaction completion at equilibrium, the emission intensities recorded, when combined

DOI: 10.1021/acsomega.7b01795
ACS Omega 2017, 2, 8618−8624

with fluorescence quantum yields for the emissive products obtained and with their fluorescence decay rate constant values k_{dec} (or their reciprocal, fluorescence decay lifetimes τ_{dec}), may provide a quantitative yield of the product formed in our palette upon the reaction with nucleophiles without the need of product isolation. Specifically, by measuring the apparent emission quantum yield (Φ_f^{app}) of solutions of **1**−**5** in 1.09 M methanol with *p*-TsOH (0.333 mM) and estimating the actual emission quantum yield of the hemiacetals formed (Φ_f), one may estimate the product yield of hemiacetal, a transient species, from the ratio of the above two values, that is, yield = Φ_f^{app}/Φ_f.

Comparison of the fluorescence of the solutions of **1**−**5** in 1.09 M methanol and *p*-TsOH, with the fluorescence from the solutions of standard compounds whose emission quantum yield is known (specifically ethyl-substituted PM605 and the analogous H-substituted dye),[18] yielded values of Φ_f^{app} for our palettes **1**−**5** in methanol (see Table 1). Although it is not possible to isolate a hemiacetal and directly measure its emission quantum yield, we obtained this parameter utilizing eq 3 by assuming that the radiative decay rate constant for these compounds is comparable to that of their *meso*-hydroxymethyl BODIPY analogues[18] (i.e., $k_{rad} \approx 1 \times 10^8$ s^{-1}) and by incorporating the τ_{dec} values measured for solutions of **1**−**5** in the presence of 1.09 M methanol and *p*-TsOH (Table 1). It is safe to estimate $k_{rad} \approx 1 \times 10^8$ s^{-1} for hemiacetals considering that similar k_{rad} values were recorded for all *meso*-hydroxymethyl BODIPY analogues of compounds **1**−**5** and for compound **6** (Table S1). This value is also typically reported in the literature for BODIPY dyes.[18,32] Tables 1 and 2 list yields of reactions based on τ_{dec} and Φ_f^{app} for solutions of compounds **1**−**5** in methanol and *p*-TsOH and also for compound **3** in the presence of various alcohols, water, and ethanedithiol and in the presence of *p*-TsOH.

Table 1. Photophysical Properties of Reaction Mixtures for Dyes 1−5 with 1.09 M Methanol in Acetonitrile and 0.333 mM *p*-TsOH[a]

dye	τ_{dec} (ns)[b]	Φ_f^{app}	Φ_f[c]	percent yield[d]
1	3.29	0.0013	0.329	0.41
2	2.00	0.0036	0.197	1.8
3	3.76 (76%), 2.08 (24%)	0.0075	0.330	2.3
4	4.14	0.015	0.406	3.8
5	2.32 (62%), 0.96 (38%)	0.012	0.177	6.9

[a]Values are reported to the significant figure as dictated by the error. Calculated quantities assume k_{rad} of 10^8 s^{-1} which may introduce a systematic error. [b]Weights of biexponential lifetimes are given based on their pre-exponential factors based on the amplitude. [c]Quantum yield was calculated from τ_{dec} and an assumed k_{rad} of 10^8 s^{-1} using eq 3 which may introduce a systematic error. An average τ_{dec} based on the weights of the pre-exponential factors was used for biexponential lifetimes (eq 4). [d]Yield was calculated from the ratio of Φ_f^{app} and Φ_f.

Table 2. Photophysical Properties of Reaction Mixtures of Dye 3 in the Presence of 1.09 M Nucleophile (Nu) in Acetonitrile and 0.333 mM *p*-TsOH[a]

Nu	T (ns)[b]	Φ_f^{app}	Φ_f[c]	percent yield[d]
MeOH	3.76 (76%), 2.08 (24%)	0.0075	0.330	2.3
EtOH	4.03 (83%), 2.39 (17%)	0.0077	0.368	2.1
BuOH	4.28 (78%), 2.61 (22%)	0.0090	0.383	2.4
EtyGly	4.20 (78%), 2.43 (22%)	0.0088	0.368	2.4
H_2O	5.34 (64%), 2.3 (36%)	0.0006	0.42	0.14
$Et(SH)_2$	4.94 (47%), 0.70 (53%)	0.050	0.264	18

[a]Values are reported to the significant figure as dictated by the error. Calculated quantities assume k_{rad} of 10^8 s^{-1} which may introduce a systematic error. [b]Weights of biexponential lifetimes are given based on their pre-exponential factors based on the amplitude. [c]Quantum yield was calculated from τ_{dec} and an assumed k_{rad} of 10^8 s^{-1} using eq 3 which may introduce a systematic error. An average τ_{dec} based on the weights of the pre-exponential factors was used for biexponential lifetimes (eq 4). [d]Yield was calculated from the ratio of Φ_f^{app} and Φ_f.

$$\Phi_f = k_{rad} \times \tau_{dec} \quad (3)$$

$$\tau_{avg} = \frac{\%_1\tau_1 + \%_2\tau_2}{100} \quad (4)$$

The above yield estimations based on photophysical properties assumed that a sole product was formed; however, should an acetal and a hemiacetal coexist, their intrinsic fluorescence lifetimes and emission quantum yields would enable a similar analysis, decoupling their contributions to the overall emission recorded and providing a direct readout on the yield of each compound.

Importantly, we found that the hemiacetals formed from the symmetric BODIPYs (**1**, **2**, and **4**) gave monoexponential lifetimes, whereas hemiacetals formed from the asymmetric BODIPYs (**3** and **5**) gave biexponential lifetimes as did compound **6** (Table S1). The two-component lifetimes for **3**, **5**, and **6** may be rationalized by the formation of atropisomers. The *meso*-position of the BODIPY core is sterically crowded because of the methyl groups at positions C1 and C7. This crowding has been shown to give rise to atropisomers from asymmetric BODIPYs.[33] Because the BODIPY core is asymmetric in compounds **3**, **5**, and **6** and the *meso*-position of BODIPY is sterically hindered (preventing rotation), formation of two atropisomers is a plausible outcome. In our analysis, we considered an average fluorescence decay lifetime based on the pre-exponential factors (amplitude) to estimate the yield for the atropisomer formation.

CONCLUSIONS

We have described herein a simple and rapid method and ensuing analysis for characterizing the reaction of nucleophiles with a series of fluorogenic *meso*-formyl BODIPY dyes. Our off/on fluorogenic reactivity palette relies on the nucleophilic addition to the formyl moiety that transforms the otherwise nonemissive *meso*-formyl BODIPY into an emissive *meso*-hemiacetal BODIPY. Our reactivity palette shows an LFER between the reactivity and the oxidation potentials of the *meso*-formyl BODIPY dyes used, where the negative slope retrieved implies an acid-catalyzed reaction. In turn, an LFER with a positive correlation between reduction potentials and reaction yield (proportional to the equilibrium constant under our experimental conditions) highlights the product stabilization with lowering of the LUMO of the reacting electrophile. The lifetimes and apparent quantum yields recorded for the palette upon reaction with nucleophiles allow for an estimation of the reaction yield of the transient hemiacetal species and the number and types of fluorescent products formed without the need for product isolation. In general, we anticipate that the analysis described herein will be of broad application to fluorescence-based assays especially when the formation of more than one product is expected.

DOI: 10.1021/acsomega.7b01795
ACS Omega 2017, 2, 8618−8624

EXPERIMENTAL SECTION

Materials. High-performance liquid chromatography grade solvents for spectroscopy were purchased from Fisher Scientific. 8-Acetoxymethyl-2,6-diethyl-1,3,5,7-tetramethyl-pyrromethene fluoroborate (PM605) was purchased from Exciton, Inc. (Dayton, OH). All other chemicals were purchased from Sigma-Aldrich, Co. and were used without further purification.

Instrumentation. Absorption spectra were recorded using a Hitachi U-2800 UV−vis−NIR spectrophotometer. Luminescence spectra were recorded using a PTI QuantaMaster spectrofluorometer using 1 cm × 1 cm quartz cuvettes and corrected for detector sensitivity. ^{1}H NMR and ^{13}C NMR spectra were recorded on a Varian VNMRS 500 instrument at 500 and 126 MHz, respectively. Electrospray ionization (ESI) mass spectra were measured on a Thermo Scientific Exactive Orbitrap.

Time-Based Fluorescent Enhancements. Time-based fluorescent measurements were recorded on a PTI QuantaMaster spectrofluorometer equipped with a four-position Peltier with motorized turret. Glass fluorimetry cells (3 mL) with 1 cm path lengths were used as sample cells. The excitation and emission slits were set to 2 nm. The temperature control was set to 21 °C. Solutions of dyes **1**−**5** in acetonitrile (3 mL final volume) were prepared in cuvettes at concentrations such that each solution had an absorbance of 0.1 at the excitation wavelength (i.e., 16, 20, 4.5, 16, and 3 μM for dyes **1**−**5**, respectively). Each solution was supplemented with 0.333 mM *p*-TsOH (unless otherwise indicated). When ready to measure intensity over time, the nucleophile of interest (1.09 M, unless otherwise specified) was added to each cuvette (final volume 3 mL). Compounds **1**, **3**, and **4** were excited at 500 nm, and their emission was collected at 560 nm. Compounds **2** and **5** were excited at 475 nm, and their emission was collected at 538 nm. The emission was background-corrected with an acetonitrile blank.

Fluorescence Quantum Yield. Acetonitrile solutions of *meso*-acetoxymethyl BODIPY dyes:[18] H_2BOAc (8-acetoxymethyl-1,3,5,7-tetramethyl pyrromethene fluoroborate) or PM605 was used as a standard to calculate the apparent quantum yields of reaction mixtures of dyes **1**−**5** in acetonitrile treated with 1.09 M methanol and 0.333 mM *p*-TsOH (following the equilibration monitored via fluorescent enhancement). *meso*-Hydroxymethyl BODIPY dye, HCNBOH (8-hydroxymethyl-2-cyano-1,3,5,7-tetramethyl pyrromethene fluoroborate),[18] was used as a standard to calculate the quantum yield of **6** in acetonitrile. Absorption and emission spectra of the standards and **6** were measured at five different concentrations. Because the fluorescence of **1**−**5** is very sensitive to concentration, only single emission and absorbance spectra were measured, following the reaction completion. The integrated emission intensity versus absorbance was then plotted and fitted linearly. Relative apparent quantum yields of fluorescence for reaction mixtures of dyes **1**−**5** and the quantum yield of dye **6** with respect to the standard were obtained from eq 5, where Φ_x, Δ, and η refer to the fluorescence quantum yield, the slope obtained from the above-mentioned plot, and the solvent refractive index for the unknown (x) or standard (st) sample, respectively.

Emission spectra were recorded for solutions using excitation and emission slits of 1.4 nm.

$$\Phi_x = \Phi_{st}\left(\frac{\Delta_x}{\Delta_{st}}\right) \times \left(\frac{\eta_x^2}{\eta_{st}^2}\right) \quad (5)$$

Fluorescence Lifetime Studies. The fluorescence lifetime measurements were carried out using a Picoquant FluoTime 200 Time-Correlated Single Photon Counting setup employing a supercontinuum laser (WhiteLase SC400-4, Fianium, Beverly, MA). Excitation wavelengths were spectrally separated from the broadband emission by a computer-controlled acousto-optical tunable filter (Fianium). Compounds **2**, **5**, and **6** were excited at 475 nm, and compounds **1**, **3**, and **4** were excited at 500 nm. The excitation rate was 10 MHz, and the detection frequency was less than 100 kHz. Photons were collected at the magic angle. An instrument response function was measured with colloidal silica beads and was used to deconvolute the time profile of the excitation source from the emission decay. Reduced chi-squared statistics were employed to determine good fits to biexponential decays.

Synthesis. Compounds **1**−**5** were prepared according to literature procedures[18] where spectroscopic data matched those of the reported materials.

*8-(1,3-Dioxolane)-2-cyano-1,3,5,7-tetramethyl Pyrromethene Fluoroborate (**6**).* Compound **5** (50 mg, 0.17 mmol) was dissolved in dry toluene (5 mL) under argon. Ethylene glycol (0.5 mL) and *p*-TsOH (3 mg, 0.015 mmol, 0.09 equiv) were added, and the solution was stirred for 4 days at 80 °C. The solution was then diluted with ethyl acetate, washed two times with saturated sodium bicarbonate, and washed once with brine. The organic layer was dried over anhydrous sodium sulfate, and the solvent was removed under reduced pressure. The title compound was purified using flash column chromatography with hexanes/ethyl acetate (1:1) giving an orange residue (9.5 mg, 17%). ^{1}H NMR (500 MHz; $CDCl_3$): δ 6.27 (s, 1H), 6.02 (s, 1H), 4.27−4.24 (m, 2H), 4.06−4.03 (m, 2H), 2.62 (s, 3H), 2.59 (s, 3H), 2.44 (s, 3H), 2.40 (s, 3H). ^{13}C NMR (126 MHz; $CDCl_3$): δ 164.9, 154.6, 147.6, 141.7, 136.9, 136.4, 129.4, 126.3, 115.2, 104.0, 98.1, 77.2, 65.0, 17.3, 15.52, 15.45, 13.6. HRMS (ESI): for $C_{17}H_{17}N_3O_2BF_2$ (M − H) calcd, 344.13874; found, 344.13933.

ASSOCIATED CONTENT

Supporting Information

The Supporting Information is available free of charge on the ACS Publications website at DOI: 10.1021/acsomega.7b01795.

^{1}H NMR and ^{13}C NMR spectra and photophysical properties for compound **6** (PDF)

AUTHOR INFORMATION

Corresponding Author

*E-mail: gonzalo.cosa@mcgill.ca.

ORCID

Gonzalo Cosa: 0000-0003-0064-1345

Notes

The authors declare no competing financial interest.

ACKNOWLEDGMENTS

G.C. is grateful to the Natural Sciences and Engineering Research Council of Canada (NSERC) and the Canadian Foundation for Innovation (CFI) for funding. L.E.G. is thankful to Vanier Canada for a postgraduate scholarship; R.L. is thankful to NSERC for a postgraduate scholarship; and K.K. is

DOI: 10.1021/acsomega.7b01795
ACS Omega 2017, 2, 8618−8624

thankful to the Drug Discovery and Training Program (CIHR) for postgraduate scholarships.

REFERENCES

(1) Chan, J.; Dodani, S. C.; Chang, C. J. Reaction-based small-molecule fluorescent probes for chemoselective bioimaging. *Nat. Chem.* **2012**, *4*, 973−984.
(2) Xia, B.; Gerard, B.; Solano, D. M.; Wan, J.; Jones, G., II; Porco, J. A., Jr. ESIPT-Mediated Photocycloadditions of 3-Hydroxyquinolinones: Development of a Fluorescence Quenching Assay for Reaction Screening. *Org. Lett.* **2011**, *13*, 1346−1349.
(3) Shaughnessy, K. H.; Kim, P.; Hartwig, J. F. A Fluorescence-Based Assay for High-Throughput Screening of Coupling Reactions. Application to Heck Chemistry. *J. Am. Chem. Soc.* **1999**, *121*, 2123−2132.
(4) Dickinson, B. C.; Huynh, C.; Chang, C. J. A Palette of Fluorescent Probes with Varying Emission Colors for Imaging Hydrogen Peroxide Signaling in Living Cells. *J. Am. Chem. Soc.* **2010**, *132*, 5906−5915.
(5) Matsumoto, T.; Urano, Y.; Takahashi, Y.; Mori, Y.; Terai, T.; Nagano, T. In Situ Evaluation of Kinetic Resolution Catalysts for Nitroaldol by Rationally Designed Fluorescence Probe. *J. Org. Chem.* **2011**, *76*, 3616−3625.
(6) Liu, J.-B.; Liu, L.-J.; Dong, Z.-Z.; Yang, G.-J.; Leung, C.-H.; Ma, D.-L. An Aldol Reaction-Based Iridium(III) Chemosensor for the Visualization of Proline in Living Cells. *Sci. Rep.* **2016**, *6*, 36509.
(7) Katsuyama, I.; Chouthaiwale, P. V.; Akama, H.; Cui, H.-L.; Tanaka, F. Fluorogenic probes for aldol reactions: tuning of fluorescence using π-conjugation systems. *Tetrahedron Lett.* **2014**, *55*, 74−78.
(8) Mase, N.; Ando, T.; Shibagaki, F.; Sugita, A.; Narumi, T.; Toda, M.; Watanabe, N.; Tanaka, F. Fluorogenic aldehydes bearing arylethynyl groups: turn-on aldol reaction sensors for evaluation of organocatalysis in DMSO. *Tetrahedron Lett.* **2014**, *55*, 1946−1948.
(9) Guo, H.-M.; Tanaka, F. A Fluorogenic Aldehyde Bearing a 1,2,3-Triazole Moiety for Monitoring the Progress of Aldol Reactions. *J. Org. Chem.* **2009**, *74*, 2417−2424.
(10) Guo, H.-M.; Minakawa, M.; Tanaka, F. Fluorogenic Imines for Fluorescent Detection of Mannich-Type Reactions of Phenols in Water. *J. Org. Chem.* **2008**, *73*, 3964−3966.
(11) Tanaka, F.; Thayumanavan, R.; Barbas, C. F. Fluorescent Detection of Carbon−Carbon Bond Formation. *J. Am. Chem. Soc.* **2003**, *125*, 8523−8528.
(12) Chen, J.; Jiang, X.; Carroll, S. L.; Huang, J.; Wang, J. Theoretical and Experimental Investigation of Thermodynamics and Kinetics of Thiol-Michael Addition Reactions: A Case Study of Reversible Fluorescent Probes for Glutathione Imaging in Single Cells. *Org. Lett.* **2015**, *17*, 5978−5981.
(13) Umezawa, K.; Yoshida, M.; Kamiya, M.; Yamasoba, T.; Urano, Y. Rational design of reversible fluorescent probes for live-cell imaging and quantification of fast glutathione dynamics. *Nat. Chem.* **2017**, *9*, 279−286.
(14) Song, F.; Garner, A. L.; Koide, K. A Highly Sensitive Fluorescent Sensor for Palladium Based on the Allylic Oxidative Insertion Mechanism. *J. Am. Chem. Soc.* **2007**, *129*, 12354−12355.
(15) Stauffer, S. R.; Hartwig, J. F. Fluorescence Resonance Energy Transfer (FRET) as a High-Throughput Assay for Coupling Reactions. Arylation of Amines as a Case Study. *J. Am. Chem. Soc.* **2003**, *125*, 6977−6985.
(16) Rozhkov, R. V.; Davisson, V. J.; Bergstrom, D. E. Fluorogenic Transformations Based on Formation of C−C Bonds Catalyzed by Palladium: An Efficient Approach for High Throughput Optimizations and Kinetic Studies. *Adv. Synth. Catal.* **2008**, *350*, 71−75.
(17) Lincoln, R.; Greene, L. E.; Bain, C.; Flores-Rizo, J. O.; Bohle, D. S.; Cosa, G. When Push Comes to Shove: Unravelling the Mechanism and Scope of Nonemissive meso-Unsaturated BODIPY Dyes. *J. Phys. Chem. B* **2015**, *119*, 4758−4765.
(18) Krumova, K.; Cosa, G. Bodipy Dyes with Tunable Redox Potentials and Functional Groups for Further Tethering: Preparation, Electrochemical, and Spectroscopic Characterization. *J. Am. Chem. Soc.* **2010**, *132*, 17560−17569.
(19) LoPachin, R. M.; Gavin, T.; Petersen, D. R.; Barber, D. S. Molecular Mechanisms of 4-Hydroxy-2-nonenal and Acrolein Toxicity: Nucleophilic Targets and Adduct Formation. *Chem. Res. Toxicol.* **2009**, *22*, 1499−1508.
(20) Perluigi, M.; Coccia, R.; Butterfield, D. A. 4-Hydroxy-2-Nonenal, a Reactive Product of Lipid Peroxidation, and Neurodegenerative Diseases: A Toxic Combination Illuminated by Redox Proteomics Studies. *Antioxid. Redox Signaling* **2012**, *17*, 1590−1609.
(21) Galligan, J. J.; Rose, K. L.; Beavers, W. N.; Hill, S.; Tallman, K. A.; Tansey, W. P.; Marnett, L. J. Stable Histone Adduction by 4-Oxo-2-nonenal: A Potential Link between Oxidative Stress and Epigenetics. *J. Am. Chem. Soc.* **2014**, *136*, 11864−11866.
(22) Avonto, C.; Chittiboyina, A. G.; Rua, D.; Khan, I. A. A fluorescence high throughput screening method for the detection of reactive electrophiles as potential skin sensitizers. *Toxicol. Appl. Pharmacol.* **2015**, *289*, 177−184.
(23) Lincoln, R.; Greene, L. E.; Zhang, W.; Louisia, S.; Cosa, G. Mitochondria Alkylation and Cellular Trafficking Mapped with a Lipophilic BODIPY−Acrolein Fluorogenic Probe. *J. Am. Chem. Soc.* **2017**, *139*, 16273−16281.
(24) Wenkert, E.; Goodwin, T. E. 4-Formyl-2-cyclohexenone derivatives. *Synth. Commun.* **1977**, *7*, 409−415.
(25) Mansilla, H.; Regás, D. Simple Method for the Preparation of Dimethyl Acetals from Ketones with Montmorillonite K 10 and *p*-Toluenesulfonic Acid. *Synth. Commun.* **2006**, *36*, 2195−2201.
(26) Öhrlein, R.; Schwab, W.; Ehrler, R.; Jäger, V. 3-Nitropropanal and 3-nitropropanol: preparation of the parent compounds and derivatives. *Synthesis* **1986**, *1986*, 535−538.
(27) Edwards, J. O. Correlation of relative rates and equilibria with a double basicity scale. *J. Am. Chem. Soc.* **1954**, *76*, 1540−1547.
(28) Loudet, A.; Burgess, K. BODIPY dyes and their derivatives: syntheses and spectroscopic properties. *Chem. Rev.* **2007**, *107*, 4891−4932.
(29) Guthrie, J. P. Hydrolysis of esters of oxy acids: pKa values for strong acids; Brønsted relationship for attack of water at methyl; free energies of hydrolysis of esters of oxy acids; and a linear relationship between free energy of hydrolysis and pKa holding over a range of 20 pK units. *Can. J. Chem.* **1978**, *56*, 2342−2353.
(30) Eckert, F.; Leito, I.; Kaljurand, I.; Kütt, A.; Klamt, A.; Diedenhofen, M. Prediction of acidity in acetonitrile solution with COSMO-RS. *J. Comput. Chem.* **2009**, *30*, 799−810.
(31) Wuts, P. G. M.; Greene, T. W. *Greene's Protective Groups in Organic Synthesis*; John Wiley & Sons, Inc., 2006; pp 431−532.
(32) Durantini, A. M.; Greene, L. E.; Lincoln, R.; Martínez, S. R.; Cosa, G. Reactive Oxygen Species Mediated Activation of a Dormant Singlet Oxygen Photosensitizer: From Autocatalytic Singlet Oxygen Amplification to Chemicontrolled Photodynamic Therapy. *J. Am. Chem. Soc.* **2016**, *138*, 1215−1225.
(33) Kolemen, S.; Cakmak, Y.; Kostereli, Z.; Akkaya, E. U. Atropisomeric Dyes: Axial Chirality in Orthogonal BODIPY Oligomers. *Org. Lett.* **2014**, *16*, 660−663.

DOI: 10.1021/acsomega.7b01795
ACS Omega 2017, 2, 8618−8624